Uncertainty quantification and propagation of crowd behaviour effects on pedestrian-induced vibrations of footbridges

Xinxin Wei[2], Jin-Cheng Liu[3], Sifeng Bi[1,*]

[1]School of Aerospace Engineering, Beijing Institute of Technology, No. 5, Zhongguancun South Street, Beijing 100081, China

[2]Ruhr-Universität Bochum, Universitätsstraße 150, D-44780 Bochum, Germany

[3]Department of Civil Engineering, The University of Hong Kong, Pokfulam, Hong Kong, China

ABSTRACT

The reliable prediction of pedestrian-induced vibration is essential for vibration serviceability assessment and further vibration mitigation design of footbridges. The response of the footbridge is governed by not only the structure dynamic model but also the crowd-induced load, which naturally involves randomness and uncertainty. It is consequently significant to appropriately characterize the uncertainties during the numerical modelling of the crowd behaviour effects on crowd-induced load. This work proposes a comprehensive approach to quantify the uncertainty from both the structure dynamic model and the crowd behaviour, and subsequently, to propagate the multiple sources of uncertainties from the input parameters to the response of the footbridge. The crowd behaviour is simulated using the social force model and translated to the crowd-induced load by combining with a single pedestrian induced walking force model. By decoupling the continuous model into several single degrees of freedom systems according to relevant modes in the vibration serviceability evaluation, the structure dynamic model of the footbridge is developed where the structural responses are calculated. In this paper, all the uncertain parameters are investigated together in a double-loop framework to perform uncertainty quantification and propagation in the form of probability-box (shortly termed as P-box). The uncertainty space of the peak structural responses is finally obtained by the Monte Carlo sampling and optimization in the outer loop and inner loop, respectively. Feasibility and performance of the overall approach are demonstrated by considering a real scale footbridge, and the failure probability of each comfort class regarding the peak acceleration response is also evaluated. Results show that, special attention should be paid on both the epistemic and aleatory uncertainties from the crowd behaviour in the vibration serviceability assessments of footbridges. The proposed uncertainty quantification framework may provide significant insights and improve the reliability for future vibration serviceability evaluations of footbridges by incorporating the crowd behaviour effects.

Keywords: human-induced vibrations; footbridges; vibration serviceability; crowd behaviour; social force model; uncertainty quantification; uncertainty propagation

1. Introduction

Modern footbridges are sensitive to human-induced excitations (Živanović et al. 2005, Gong et al. 2021). When the vibration serviceability criteria are not satisfied, vibration mitigation measures are required (e.g., Diaz and Reynolds 2010, and Ferreira et al. 2019). In dynamic design of footbridges, vibration serviceability is satisfied by controlling the predicted vibration levels within comfort levels required by users and guidelines (HiVoSS 2008, Sétra 2006, and ISO 10137, 2007). Comfort levels in guidelines are commonly defined as limiting

* Corresponding author.
Email address: **sifeng.bi@bit.edu.cn** (Sifeng Bi)

accelerations. The reliable prediction of structural responses is essential for vibration serviceability assessment and further vibration mitigation design of footbridges if relevant.

The response of the footbridge is governed by not only the structure dynamic model but also the crowd-induced load (Wei et al. 2017 and Fu and Wei 2020). Sources of uncertainties exist in the prediction of pedestrian-induced vibrations of footbridges both for the structure and excitation parts. For the structure part, the natural frequencies may be variant due to environmental changes e.g., temperature and humidity (e.g., Xia et al. 2006, Moser and Moaveni 2011, and Borges et al. 2021). Damping ratios are also inherently uncertain (e.g., Kareem and Gurley 1996 and Geweth et al. 2021). Furthermore, due to the mechanical interaction between the pedestrian crowd and the structure (the so-called human-structure interaction, HSI), the dynamic parameters of the coupled crowd-structure system can be significantly modified when compared to the empty structure before the arrival of the pedestrians (e.g., Alexander 2006 and Mohammed and Pavic 2020). Basically, researchers agree that, the HSI can add damping to the coupled system and the modal frequencies can be slightly modified. Lievens et al. (2016) investigated the effect of modal parameter uncertainties on the predicted structural responses. More specifically, it reports that, the deviation from the nominal value can be up to 10% for natural frequency; the deviation can be up to 50% for damping ratio. Based on the vibration serviceability assessment of real footbridges, it shows that, the modal parameter uncertainties significantly affect the prediction results.

Considering the human-induced excitation loaded on the footbridge, significant sources of the crowd-induced load include: crowd density, arrival times, pedestrian walking speeds, walking trajectories, step frequencies, body weights, etc. For the crowd density, current guidelines (e.g., HiVoSS 2008 and Sétra 2006) suggest considering six typical densities in the design, i.e., 0.1, 0.2, 0.5, 0.8, 1.0, 1.5 persons/m^2. To consider the randomness of arrival times, a Poisson distribution is generally employed (Živanović 2012). The importance of considering the inter- and intra-subject variabilities in walking speeds, walking trajectories, step frequencies, and body weights in the prediction of structural responses are investigated by recent research (e.g., Wei et al. 2017 and Fu and Wei 2020). Results also show it is essential to consider crowd behaviour effects in the prediction of pedestrian-induced vibrations.

However, to the best of the authors' knowledge, few works directly applies uncertainty quantification methodology to account for crowd behaviour effects, and thus few relevant investigations is performed on how the uncertainties propagate and how much the uncertainties affect the pedestrian-induced responses of the footbridge. Uncertainty quantification and propagation have been widely investigated in various engineering fields such as, probabilistic model updating (Behmanesh et al. 2018) of and reliability analysis (Jiang et al. 2021, Zhang 2005 and Zhang et al. 2010) of civil structures, parameter estimation of ultrasonic inspection system (Ben Abdessalem et al. 2018), precise numerical modelling of aerospace structures (Vishwanathan and Vio 2019), and performance assessment of heavy-duty vehicle system (Kwon 2020), etc.

The uncertainty quantification and propagation approaches allow the numerical simulation to be extended from the deterministic domain to the stochastic domain, where the predicted system responses are regarded as imprecisely probabilistic variables that fall into the uncertainty space. In this work, the uncertainty space is characterized by the conception *probability-box*, shortly termed as P-box, (Bi et al. 2019) where both the aleatory uncertainty and the epistemic uncertainty are considered. As a classical categorization approach, the uncertainties are divided to be either aleatory or epistemic according to it is caused either by the natural randomness of the system, or caused by the lack of knowledge. In current study, all the uncertain parameters of the structure dynamic model and the crowd-induced load of the footbridge are investigated together and classified into four categories according to whether the aleatory and/or epistemic uncertainties are involved. The P-boxes are calculated for each of the four categories of input parameters, and subsequently propagated through a double-loop framework, after which the P-box of the system response of the footbridge, i.e. the maximum acceleration responses, is obtained. The double-loop approach is motivated from the interval Monte Carlo method for reliability analysis proposed by Zhang et al. (2010). This approach investigates the aleatory uncertainty and the epistemic uncertainty separately, where the aleatory uncertainty is characterized by specific distribution of the parameter, while the epistemic uncertainty is presented by assuming the distribution coefficients as unknown-but-bounded values. The reliability analysis therefor considers families of distributions whose parameters are within the intervals. Correspondingly, the failure probability is no longer a determined value but an uncertain value fallen within an interval. Being different from the interval Monte Carlo methods, this work proposes a double-loop approach where the outer loop employs the Monte Carlo sampling approach, and the inner loop employs the optimization to search the epistemic uncertainty space. The double-loop allows the propagation of the uncertainty from the input parameters to the output features. As a result, the P-box of the system behaviours, such as the human-induced vibration, is available.

The P-box of the human-induced vibration provides an effective means to estimate confidence for the predicted structural responses of the footbridge. For instance, the range of the failure probability regarding the peak vibration response can be assessed. From the aspect of engineering practices of the vibration serviceability analysis, it is essential to provide references for footbridge designers with the information on the maximum acceleration responses, such that to avoid the design to be either too risky or conservative.

The proposed approaches and the remaining parts of the paper are explained as follows. Section 2 presents the social force model to characterize the crowd behaviours, i.e. the time-variant position and velocity of pedestrians, which are subsequently translated into the crowd-induced load. Section 3 develops the structural responses calculation of the footbridge excited by the above obtained crowd-induced load, through a linear dynamic system with proportional damping. The double-loop uncertainty quantification and propagation framework are formulated in Section 4, where the Monte Carlo technique and optimization are performed in the outer and inner loops, respectively. Section 5 presents an illustrative example. Finally, conclusions are drawn in Section 6.

2. Representation of crowd-induced load

2.1 Crowd behaviour simulation

In a pedestrian crowd, there are necessarily different pedestrians. Different persons may inevitably have different walking parameters and induce different walking forces, i.e. the so-called inter-person variability. Even for a single person, he/she can also walk in different ways and thus results in different walking parameters and loads. This is the intra-person variability (Živanović et al. 2005 and Fu and Wei 2020). To consider the inter- and intra-person variability in walking parameters and induced forces among pedestrians in a crowd, the pedestrian crowd model is required to consider the individual and microscopic crowd behaviour. Furthermore, to reliably predict the pedestrian-induced vibrations of footbridges, it also requires knowing relevant crowd behaviour such as passing trajectories and speeds of each pedestrian in the crowd (e.g., Wei et al. 2017 and Fu and Wei 2020). When passing on a structure, the crowd behaviour is influenced not only by their personal motivation and psychological effects, but also the interactions with their surroundings, i.e. other people in the crowd and obstacles in the walkway. Mathematically, all these influencing factors can be treated as forces acting on and guiding each person in the crowd (Helbing et al. 1995, 2000a, 2005).

Due to its ease of use and its effectiveness to capture the main characteristics of crowd behaviour, the social force model becomes one of the most widely applied models to simulate pedestrian crowd behaviour on pedestrian structures (Helbing et al. 1995, 2000a, 2005, Wei et al. 2017 and Fu and Wei 2020). The basic idea is that each person (represented by a randomly selected pedestrian α) in a crowd is guided by the social force composed of three force items. To be simplified and uniform for all persons, the force items [N] are expressed in terms of acceleration [m/s^2], which can be easily converted to force by multiplying the corresponding body mass m_α [kg]. The three force items, namely the driving force, the repulsive force subject to collision, and the repulsive force subject to borders, are explained as follows.

(1) The driving force

A driving item to motivate the person to the desired destination:

$$\vec{f}_\alpha^0(t) = [\, v_\alpha^0(t)\vec{e}_\alpha(t) - \vec{v}_\alpha(t)\,]/\tau_\alpha \tag{1}$$

which is dependent on the desired speed $v_\alpha^0(t)$, the desired direction $\vec{e}_\alpha(t)$, the actual velocity $\vec{v}_\alpha(t)$, and the relaxation time $\tau_\alpha = 0.5$ s (Helbing et al. 1995, 2000a and Wei et al. 2017). The relaxation time is the time required to eliminate the difference between the actual and the desired velocities. The desired speed is time-variant and shows an increasing trend, which can be considered as:

$$v_\alpha^0(t) = [1 - n_\alpha(t)]\, v_\alpha^0(0) + n_\alpha(t) v_\alpha^{max} \tag{2}$$

In which, $v_\alpha^0(0)$ and $v_\alpha^{max}(= 1.3 \times v_\alpha^0(0))$ are the initial and maximum desired walking speeds, respectively. $n_\alpha(t)$ is a quantity to reflect the person's nervousness and impatience in the walking process to attain the desired destination:

$$n_\alpha(t) = 1 - \bar{v}_\alpha(t)/\, v_\alpha^0(0) \tag{3}$$

with $\bar{v}_\alpha(t)$ the average walking speed.

(2) The repulsive force subject to collision

A repulsive item is considered to avoid collision with or try to keep a certain distance from others. This force is mainly due to psychological effect. To illustrate it, another random person (pedestrian β) in the crowd is introduced. The interaction force between the pedestrian α and β is:

$$\vec{f}_{\alpha\beta}(t) = A_\alpha^1 e^{\frac{r_{\alpha\beta} - d_{\alpha\beta}}{B_\alpha^1}} \vec{n}_{\alpha\beta}[\lambda_\alpha + (1 - \lambda_\alpha)\frac{1 + \cos(\emptyset_{\alpha\beta})}{2}] \tag{4}$$

with two parameters related to the territorial effect $A_\alpha^1 = 9.43$ m/s^2 (the interaction strength) and $B_\alpha^1 = 0.35$ m (the repulsive interaction range) (Wei et al. 2017 and Wei 2021). $r_{\alpha\beta} = r_\alpha + r_\beta = 0.6$ m is the sum of the two pedestrian radii (Helbing et al. 1995, 2000a). The radii of the two persons can be assumed as the same, i.e., $r_\alpha = r_\beta = 0.3$ m. $d_{\alpha\beta}$ is the distance between these two mass centres. $\lambda_\alpha = 0.82$ is a factor to account for the anisotropic nature of the pedestrian interaction (Wei et al. 2017 and Wei 2021). The anisotropic nature refers to the fact that, the walking person is influenced by more the front pedestrians than the persons behind. $\vec{n}_{\alpha\beta}$ is the normalized vector directing from the pedestrians β towards α, which depends on the locations $\vec{r}_\alpha(t)$ and $\vec{r}_\beta(t)$ of the two persons:

$$\vec{n}_{\alpha\beta} = \frac{\vec{r}_\alpha(t) - \vec{r}_\beta(t)}{d_{\alpha\beta}(t)} \tag{5}$$

Furthermore, $\emptyset_{\alpha\beta}$ is the angle between the vector $\vec{n}_{\alpha\beta}$ and the direction $\vec{e}_\alpha(t)$:

$$\cos\emptyset_{\alpha\beta}(t) = -\vec{n}_{\alpha\beta}(t)\cdot\vec{e}_{\alpha}(t) \tag{6}$$

In a real crowd, all neighbouring pedestrians contribute the interaction force acting on the pedestrian α, i.e., the total interaction force is $\sum_{\beta\neq\alpha}^{n_p}\vec{f}_{\alpha\beta}(t)$, with n_p the total number of involved pedestrians, but the force contributions only come from the other n_p-1 persons since the pedestrian α him/herself does not have such force item.

(3) The repulsive force subject to borders

Another repulsive item is to keep clear from borders, e.g., obstacles in the walkway and boundaries of the walking area. The illustration is provided by considering a random border B:

$$\vec{f}_{\alpha B}(t) = A_{\alpha}^{B}e^{\frac{r_\alpha-d_{\alpha B}}{B_{\alpha}^{B}}}\vec{n}_{\alpha B} \tag{7}$$

with the interaction strength $A_{\alpha}^{B}=5$ m/s² and the repulsive interaction range $B_{\alpha}^{B}=0.1$ m due to borders (Helbing et al. 2000a and 2005). $d_{\alpha B}(t)$ is the distance between the mass centre of the pedestrian α and the nearest point of the border; $\vec{n}_{\alpha B}(\mathrm{t})$ is the normalized vector directing from the nearest point of the border to the pedestrian α:

$$\vec{n}_{\alpha B}(\mathrm{t}) = \frac{\vec{r}_{\alpha}(t)-\vec{r}_{B}(t)}{d_{\alpha B}(t)} \tag{8}$$

As a sum, the interaction forces with borders are $\sum_{B}^{n_B}\vec{f}_{\alpha B}(t)$. n_B is the number of borders involved.

Thus, the total social force acting on the pedestrian α is

$$\vec{f}_{\alpha}(t) = \vec{f}_{\alpha}^{0}(t) + \sum_{\beta\neq\alpha}^{n_p}\vec{f}_{\alpha\beta}(t) + \sum_{B}^{n_B}\vec{f}_{\alpha B}(t) \tag{9}$$

To better illustrate the social force model acting on the pedestrian α, a visualized plot is presented in Fig. 1. Guided by the social force, the time-variant position $\vec{r}_{\alpha}(t)$ and velocity $\vec{v}_{\alpha}(t)$ of the person can be obtained by solving the set of coupled differential equations:

$$\frac{\mathrm{d}\vec{r}_{\alpha}(t)}{\mathrm{d}t} = \vec{v}_{\alpha}(t) \tag{10}$$

$$\frac{\mathrm{d}\vec{v}_{\alpha}(t)}{\mathrm{d}t} = \vec{f}_{\alpha}(t) \tag{11}$$

The equations can be solved in a time-stepping procedure. Specially, to keep a balance between the accuracy and the efficiency for the obtained positions and velocities, the time step can be set as, e.g. 0.1 s.

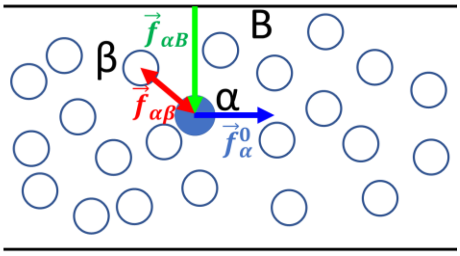

Fig. 1 Visualization for the social force model acting on the pedestrian α.

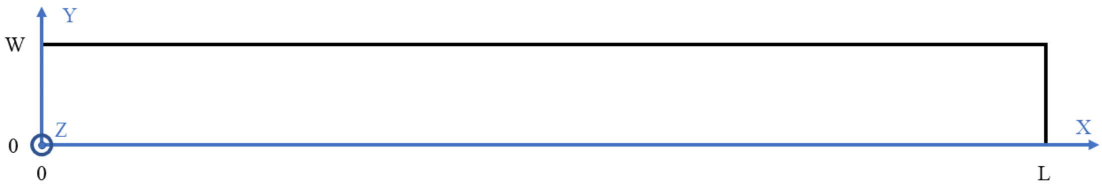

Fig. 2 The coordinate system and dimensions of the walking area on the footbridge deck. X (along the length), Y (along the width), and Z (along the height) are the longitudinal, lateral, and vertical directions, respectively.

For a given structure (Fig. 2), to simulate the possible crowd behaviour that may pass on it, the structural dimensions (width W and length L) are reasonably assumed to be constant. However, different pedestrian traffic scenarios are expected on the structure. The most relevant cases are defined as pedestrian crowds with six different densities, i.e., 0.1, 0.2, 0.5, 0.8, 1.0, 1.5 persons/m² (HiVoSS 2008 and Sétra 2006). Furthermore, for a pedestrian crowd with a given density d, three key random variables should be considered, i.e., the arrival time $t_{\mathrm{arr},\alpha}$, the initial position in lateral direction at the entrance Y_{α}^{0}, and the initial desired walking speed $v_{\alpha}^{0}(0)$. These random variables are explained as follows.

● The arrival time $t_{\mathrm{arr},\alpha}$: different pedestrians may arrive at the structure at different times. The different arrival times are expressed as a Poisson distribution (Živanović 2012, Wei et al. 2017 and Fu and Wei 2020). The probability mass function of the Poisson distribution is

$$f(x) = \frac{\lambda^{x}}{x!} \cdot e^{-\lambda}, \tag{12}$$

with $\lambda = W \cdot d \cdot \bar{v}(d)$. The pedestrian arrival rate λ [persons/s] is determined by the bridge width W, the (target) crowd density d, and the mean walking speed of the crowd $\bar{v}(d)$. The latter is variant for different geographic areas and travel purposes (Bruno and Venuti, 2008):

$$\bar{v}(d) = \alpha_{\mathrm{G}} \cdot \alpha_{\mathrm{T}} \cdot \bar{v}_{\mathrm{free}} \cdot \left\{1 - \exp\left[-\gamma \cdot \left(\frac{1}{d} - \frac{1}{d_{\mathrm{jam}}}\right)\right]\right\}, \tag{13}$$

In which, $\bar{v}_{\mathrm{free}} = 1.34$ m/s is the average free walking speed (Helbing et al. 1995, 2000a, Wei et al. 2017 and Fu and Wei 2020). α_{G} and α_{T} are adjusting coefficients to consider different geographic areas and travel purposes, respectively. Another parameter to consider the travel purposes is the adjusting coefficient γ: for the rush hour, the commuter, and the leisure purposes, $\gamma = 0.273 d_{\mathrm{jam}}$, $0.214 d_{\mathrm{jam}}$, and $0.245 d_{\mathrm{jam}}$, respectively (Bruno and Venuti, 2008). d_{jam} is jam density, which can be considered with 5.4 persons/m², as Weidmann et al.

(Bruno and Venuti, 2008, Weidmann 1993, Buchmueller and Weidmann 2006). As shown in the Table 1 and Fig. 3, basically, European people on average walk faster than people in USA and Asia; people walk slowest in leisure status and fastest in rush hour. It is also notable that, when mixed factors are considered for geographic areas and travel purposes, the comparative relationship may be changed, e.g., for most densities, Asia people in rush hour walk faster than European and American people in commuters; however, the relationship is opposite for low densities. In other words, commuter pedestrians can walk faster than rush-hour people, when different geographic areas are considered. As the aforementioned expressions, for a crowd in known geographic area and travel purpose, the corresponding Poisson distribution can be determined for given bridge width W and crowd density d.

● The initial positions in lateral (Y) direction at the entrance Y_α^0: different pedestrians start walking from different initial positions at the entrance of the walking area. To ensure safety, the body centre of each person at least keeps away from the border with a distance of the pedestrians' radii r_α ($= 0.3$ m, according to (Helbing et al. 1995, 2000a)). Thus, Y_α^0 is considered to follow a Uniform distribution: $U(r_\alpha, W - r_\alpha)$ m.

● The initial desired walking speed $v_\alpha^0(0)$: when start walking, different pedestrians may have different initial walking speeds. On average, at the free walking status, the speeds follow a Normal distribution as: $\mathcal{N}(1.34, 0.26)$ m/s (Helbing et al. 1995, 2000a, Wei et al. 2017 and Fu and Wei 2020).

Table 1: adjusting coefficients α_G and α_T.

α_G for geographic areas			**α_T for travel purposes**		
Europe	USA	Asia	Rush-hour /Business	Commuters /Events	Leisure /Shopping
1.05	1.01	0.92	1.20	1.11	0.84

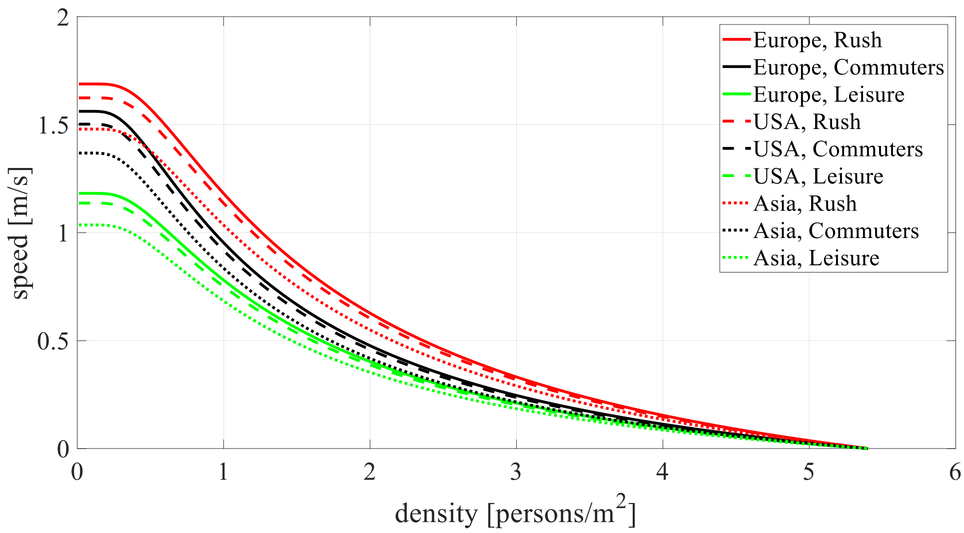

Fig. 3. The speed-density relations for pedestrian crowds at different geographic areas and travel purposes.

2.2 Translation from crowd behaviour to crowd-induced load

During the passing process of the crowd, the pedestrians excite the structure in terms of walking forces. Based on the time-variant positions and velocities of each person regulated by the social force, the loading trajectories and step frequencies of each pedestrian are determined. The loading trajectories of the walking forces are just following the walking trajectories for each person. The step frequencies of each person are obtained by the translation relation as follows (Wei et al. 2017 and Fu and Wei 2020):

$$f_{s,\alpha} = 0.35v_{s,\alpha}^3 - 1.59v_{s,\alpha}^2 + 2.93v_{s,\alpha} \tag{14}$$

By inputting the step frequencies into the walking force model of a single pedestrian, the actual walking forces acting on the structure by the person are determined. This study considers the vertical force component as (Wei et al. 2017 and Fu and Wei 2020):

$$F_{z,\alpha}(t) = G_\alpha \cdot [1 + \sum_{j=1}^{n_z} DLF_{z,\alpha,j} \cdot \sin(2\pi \cdot j \cdot f_{s,\alpha} \cdot t + \varphi_{z,\alpha,j})] \tag{15}$$

Where, the pedestrian-induced force component in vertical direction (the Z direction of the bridge deck as shown in Fig. 2) is expressed as $F_{z,\alpha}(t)$. $G_\alpha = m_\alpha \cdot g$ is the body weight. n_z is the number of harmonics. The walking force is theoretically composed of infinite harmonics, but in practice, it is usually enough to consider only the first several harmonics, which are relevant in the vibration serviceability assessments for most footbridges. It can be even more simplified: as suggested by the design guidelines (e.g., HiVoSS 2008 and Sétra 2006), the structural responses are often governed by the mode with natural frequency in the range of walking forces; and thus, it is often reasonable to only consider the relevant single mode in the vibration serviceability assessment. $DLF_{z,\alpha,j}$ is the corresponding dynamic load factor (DLF) for the jth harmonic. According (Young 2001), the DLFs are dependent on step frequency $f_{s,\alpha}$, which are defined as:

$DLF_{z,\alpha,1} = 0.41(f_{s,\alpha} - 0.95)$, for the 1st harmonic, with $f_{s,\alpha}$ in [1, 2.8] Hz; (16a)

$DLF_{z,\alpha,2} = 0.069 + 0.0056 \times 2f_{s,\alpha}$, for the 2nd harmonic, with $2f_{s,\alpha}$ in [2, 5.6] Hz; (16b)

$DLF_{z,\alpha,3} = 0.033 + 0.0064 \times 3f_{s,\alpha}$, for the 3rd harmonic, with $3f_{s,\alpha}$ in [3, 8.4] Hz; (16c)

$DLF_{z,\alpha,4} = 0.013 + 0.0065 \times 4f_{s,\alpha}$, for the 4th harmonic, with $4f_{s,\alpha}$ in [4, 11.2] Hz. (16d)

The corresponding phase angle is considered as $\varphi_{z,\alpha,j} = 0$ in the calculations, due to lack of reliable experimental data and precise physical meaning.

The time-variant crowd-induced load is constructed by superposition of the force contributions from all real-time pedestrians on the structure. The sources of randomness of the pedestrian-induced loads (directly and indirectly) come from:

- The body weight G_α: different pedestrians may have different body weights. The scatter can be described with a Normal distribution, e.g., $\mathcal{N}(750,150)$ N (Živanović 2012).
- The walking speeds $v_{s,\alpha}$: the walking speeds are determined by the parameters of the social force model (see subsection 2.1) and may affect the time history of the loading. The distributions are unknown and thus require to be determined.
- The step frequency $f_{s,\alpha}$: the step frequencies are determined by the speeds $v_{s,\alpha}$ (see Eq. (14)). The distributions are also to be determined.

• The DLFs $DLF_{z,\alpha,j}$: the DLFs are dependent on step frequency $f_{s,\alpha}$, as defined in Eq. (16). The distributions are unknown and to be given.

3. Structural response calculation

To calculate the structural responses induced by the crowd, basic assumptions as mentioned in classic dynamics of structures are applied (Chopra 2012), i.e., linear system and proportional damping are assumed. The basic equations of motion can be:

$$\mathbf{M}\ddot{\boldsymbol{Z}} + \boldsymbol{C}\dot{\boldsymbol{Z}} + \boldsymbol{K}\boldsymbol{Z} = \boldsymbol{P}(\boldsymbol{t}) \tag{17}$$

with the mass matrix $\mathbf{M}$, the damping matrix $\boldsymbol{C}$, and the stiffness matrix $\boldsymbol{K}$. $\ddot{\boldsymbol{Z}}$, $\dot{\boldsymbol{Z}}$, and $\boldsymbol{Z}$ are the acceleration, velocity, and displacement matrix, respectively. $\boldsymbol{P}(\boldsymbol{t})$ is the load matrix.

Based on the basic assumptions, the system is decoupled into n_{dof} equivalent single degree of freedom (SDOF) systems. The n_{dof} can be determined by considering the relevant modes in the vibration serviceability evaluation. For each SDOF system, it has a set of modal parameters (the modal mass M_n, natural frequency f_n and modal damping ratio D_n). The SDOF system is governed by:

$$M_n\ddot{z}_n + C_n\dot{z}_n + K_n z_n = \{\emptyset_n\}^T \boldsymbol{P}(\boldsymbol{t}) \tag{18}$$

with $C_n = 2M_n D_\mathrm{n}(2\pi f_\mathrm{n})$ and $K_n = M_n(2\pi f_\mathrm{n})^2$ the corresponding damping and stiffness coefficients, respectively. $\ddot{z}_\mathrm{n}$, $\dot{z}_\mathrm{n}$ and z_n are the modal acceleration, velocity, and displacement, respectively. $\emptyset_n$ is the corresponding vibration mode. The corresponding modal load $\{\emptyset_n\}^T \boldsymbol{P}(\boldsymbol{t})$ is obtained by superposition of the force contributions from all real-time pedestrians on the structure.

In the structural response calculation, the modal mass M_n is reasonably assumed to be constant. However, the natural frequency f_n and damping ratio D_n are expected to be variant (Xia et al. 2006, Moser and Moaveni 2011, and Lievens et al. 2016).

• To consider the corresponding scatters in f_n and D_n, the basic assumptions are made as: the f_n and D_n have nominal values $\bar{f}_n$ and $\bar{D}_n$ as the corresponding mean values, respectively. The actual values of f_n and D_n may vary and thus respectively considered as variable within intervals of $[0.9\bar{f}_n, 1.1\bar{f}_n]$ Hz and $[0.5\bar{D}_n, 1.5\bar{D}_n]$, according to observations in (Lievens et al. 2016).

4. Uncertainty quantification (UQ) framework

4.1 Uncertainty sources and parameter categorisation

Uncertainties in the prediction of pedestrian-induced vibrations of footbridges come from both the structure and the excitation parts. The former can include the structure's modal parameters (modal mass, natural frequency, and damping ratio), geometric size (length, width, …), etc. The latter covers the properties of the crowd as described in Sec. 2, including geographic area, travel purpose, the pedestrians' arrival times, initial positions, initial speeds, body weights, etc. Although the above parameters are regarded to be "uncertain", they can be governed by different types of uncertainties. The uncertainty is classified to be either epistemic or aleatory. The epistemic uncertainty is caused by lack of knowledge, and thus it can be reduced as the better understanding of the investigated problem is achieved; the aleatory uncertainty is the natural feature of the physical system which cannot be avoided; however, it still requires the appropriate representation. For example, the pedestrians' arrival times, initial positions, initial speeds, and body weights are governed by the aleatory uncertainty, while the analytical model of the structure dynamic model of the bridge involves epistemic uncertainty leading the natural frequency and damping ratio cannot be precisely determined. Note that, it is also possible that some parameters would involve both the epistemic and aleatory uncertainties simultaneously.

To perform a comprehensive uncertainty analysis involving all the uncertainty sources above, it is necessary to first categorize these parameters into four types according to whether the epistemic uncertainty or the aleatory uncertainty is involved (Bi et al. 2019).

● Type I: parameters without any uncertainty, i.e., explicit constants. For instance, for a given structure, the length and width can be regarded as fully determined constant values.

● Type II: parameters with only epistemic uncertainty. These parameters are unknown-but-fixed constants, bounded by a known interval. For example, the natural frequency and damping ratio can be variant within certain intervals.

● Type III: parameters with only aleatory uncertainty. These parameters are no longer constants but can be described as random variables. Because no epistemic uncertainty is involved, the random variable can be fully determined by its probability characteristics e.g., the distribution format, mean and variance.

● Type IV: parameters with both aleatory and epistemic uncertainties. Being more complex than the Type III and II, theses parameters are imprecise probability variables with only vaguely determined uncertainty characteristics.

Different representations of uncertainty characteristics are applied according to the corresponding categorisation of parameters. Ferson (2003) proposed the P-box to describe the uncertainty space of variables with imprecise probability, i.e., the Type IV parameters. More detailed information can be found in (Bi et al. 2019). The following text briefly introduces the most relevant contents for uncertainty quantification and propagation through the analytical model in the format of P-box.

4.2 Footbridge uncertainty behaviour quantification through P-box

The P-box is a visualized representation for uncertainty space of variables with imprecise probability. More specifically, a distributional P-box is a family of cumulative distribution functions (CDF) for a random variable, encompassing an infinite number of CDF curves. The CDF family $\mathcal{F}(p)$ for a variable p is expressed as:

$$\mathcal{F}(p) \supseteq \mathcal{F}(p,\theta),\ \ \theta \in [\underline{\boldsymbol{\theta}}, \overline{\boldsymbol{\theta}}] \tag{19}$$

with θ the distribution coefficients of p. The parameter p can be any type of the previously categorized four parameter types, which corresponds to different formats of P-boxes (Fig. 4). For the most complex case (type IV variable), the epistemic uncertainty is presented by the interval $[\underline{\boldsymbol{\theta}}, \overline{\boldsymbol{\theta}}]$. This interval leads to infinite number of CDF curves within the distributional P-box, and that is why a P-box is also known as an uncertainty space of an imprecise probability variable p. The lower and upper bounds of the curve family $\underline{\mathcal{F}}$ and $\overline{\mathcal{F}}$ can be determined by the interval of the distribution coefficients $[\underline{\boldsymbol{\theta}}, \overline{\boldsymbol{\theta}}]$. The shape (horizontal position and slope) of each CDF curve is controlled by the mean and variance of a distribution: the horizontal position is determined by the mean value; the slope is dependent on the variance value (scatter level of the distribution). More specifically, the horizontal position moves along the direction of the increase in the mean; the slope tends to gentler with the increase of the variance value. It is notable that a P-box border is not always a complete CDF curve of a specific distribution, but sometimes a combination of multiple CDF curves.

4.3 Propagation of the P-box from the input parameters to the footbridge behaviour

A double-loop approach is proposed in this subsection to propagate the uncertainty sources from the input parameters to the output behaviour of the footbridge, i.e., the pedestrian-induced vibrations, such that the uncertainty properties of the footbridge vibration can be quantified. The double-loop process is illustrated in Fig. 4, where the outer loop employs the Monte Carlo approach to handle the aleatory uncertainty, and the inner loop executes the optimization to determine the maximum and minimum of the output regarding to each Monte Carlo sampling. In the outer loop, it quantifies the aleatory uncertainty by a Monte Carlo process within the probability space of the cumulative distribution function. Specifically, in each Monte Carlo simulation, for each parameter, it randomly samples a separate probability value along the vertical direction of the P-box (Fig. 4). As shown in Fig. 4, different categories of parameters correspond to different forms P-boxes. To be clear in expressions, p_1, p_2, p_3, and p_4 are applied to represent the four types of parameters, i.e., Type I, II, III, IV, respectively. Correspondingly, α_1, α_2, α_3, and α_4 represent the probability values in a sample.

● For Type I: this type of parameter has no uncertainty and thus the CDF simply appears as an impulse function with amplitude of 1, at the fixed position with the parameter value p^*. Thus, a randomly sampled probability value α_1 corresponds to an invariant parameter value p^*.

● For Type II: due to epistemic uncertainty, this type of parameter has a family of impulse functions with the given interval $[\underline{p}^*, \overline{p}^*]$. The corresponding P-box is a standard rectangle. A random value α_2, corresponds to the known interval $[\underline{p}^*, \overline{p}^*]$.

● For Type III: the type of parameter is described by a fully determined probability distribution. Thus, each probability value α_3 is related to a separate parameter value $p^{(\alpha_3)}$. In other words, different probability values correspond to different parameter values according to the CDF curve of the distribution.

● For Type IV: for the most complex type of parameter, each probability value α_4 corresponds to a separate interval $[\underline{p}^{(\alpha_4)}, \overline{p}^{(\alpha_4)}]$. The interval is obtained during the Monte Carlo simulation.

The inner loop is performed simultaneously during the Monte Carlo simulation of the outer loop. For each sample of the Monte Carlo simulation, the inner loop is carried out to propagate the epistemic uncertainty from the inputs to the outputs, by solving an optimisation problem. The constrains of the optimisation problem are exert from the outcome of the first loop (the random set realisations). In this study, the 'random set realisations' refer to the different realisations (fixed/varying point or interval) of the parameter (Fig. 4). The inner loop deals with the epistemic uncertainty involved in the random set realisations. To be general, the problem is illustrated with an uncertain system:

$$\boldsymbol{x} = h(\boldsymbol{p}) \tag{20}$$

where, the system represents the whole simulation process, i.e., from the inputs $\boldsymbol{p}$, the simulator $h(\cdot)$, to the outputs $\boldsymbol{x}$.

The uncertainty propagation is proceeded by solving an optimisation problem to determine the minimum and maximum of the outputs. The optimisation problem is to find:

$$\min_{\boldsymbol{p}}\{\boldsymbol{x} = h(\boldsymbol{p})\} \text{ and } \max_{\boldsymbol{p}}\{\boldsymbol{x} = h(\boldsymbol{p})\} \tag{21}$$

using the random set realisations as constraints (Fig. 4), i.e.:

$$\begin{cases} p_1{}^{(\alpha_1)} = p^* \\ p_2{}^{(\alpha_2)} \in [\underline{p}^*, \overline{p}^*] \\ p_3{}^{(\alpha_3)} = p^{(\alpha_3)} \\ p_4{}^{(\alpha_4)} \in [\underline{p}^{(\alpha_4)}, \overline{p}^{(\alpha_4)}] \end{cases} \tag{22}$$

where values of the parameters with the superscript (*) are fixed, while the parameters with the superscript (α) are variant with the probability value α. It is notable that, constraints defined by Eq. (22) are simple interval constraints, i.e., no complex nonlinear constraints are involved. Furthermore, the interval constraints represent only the epistemic uncertainty, implying the ranges of the intervals are much smaller than the whole domain of definition of the parameters in the system. Thus, the optimisation problem can be solved by typical techniques, e.g., simplex algorithm and interior point method.

Fig. 4 presents the overall double loop procedure of uncertainty quantification and propagation. To be generalized, it assumes N_{MC} Monte Carlo simulations are performed in the UQ, i.e., the sampling size is N_{MC}. Correspondingly, N_{MC} random set realisations of the input parameters will be obtained in the first loop. Meanwhile, it executes N_{MC} times optimisation, with once for each random set realisation. N_{MC} pairs of minimum and maximum output values will be generated. Two CDFs can be estimated based on the N_{MC} pairs of minimum and maximum output values. The P-box of the outputs is thus bounded by the two fitted CDFs.

After the aforementioned procedures, the P-box provides a clear representation of the uncertainty space of the vibration behaviour of the footbridge. The P-box presentation makes it possible to evaluate the range of the failure probability, which is influenced by both aleatory and epistemic uncertainties from not only the footbridge dynamic model but also the uncertain crowd-induced load added on the footbridge.

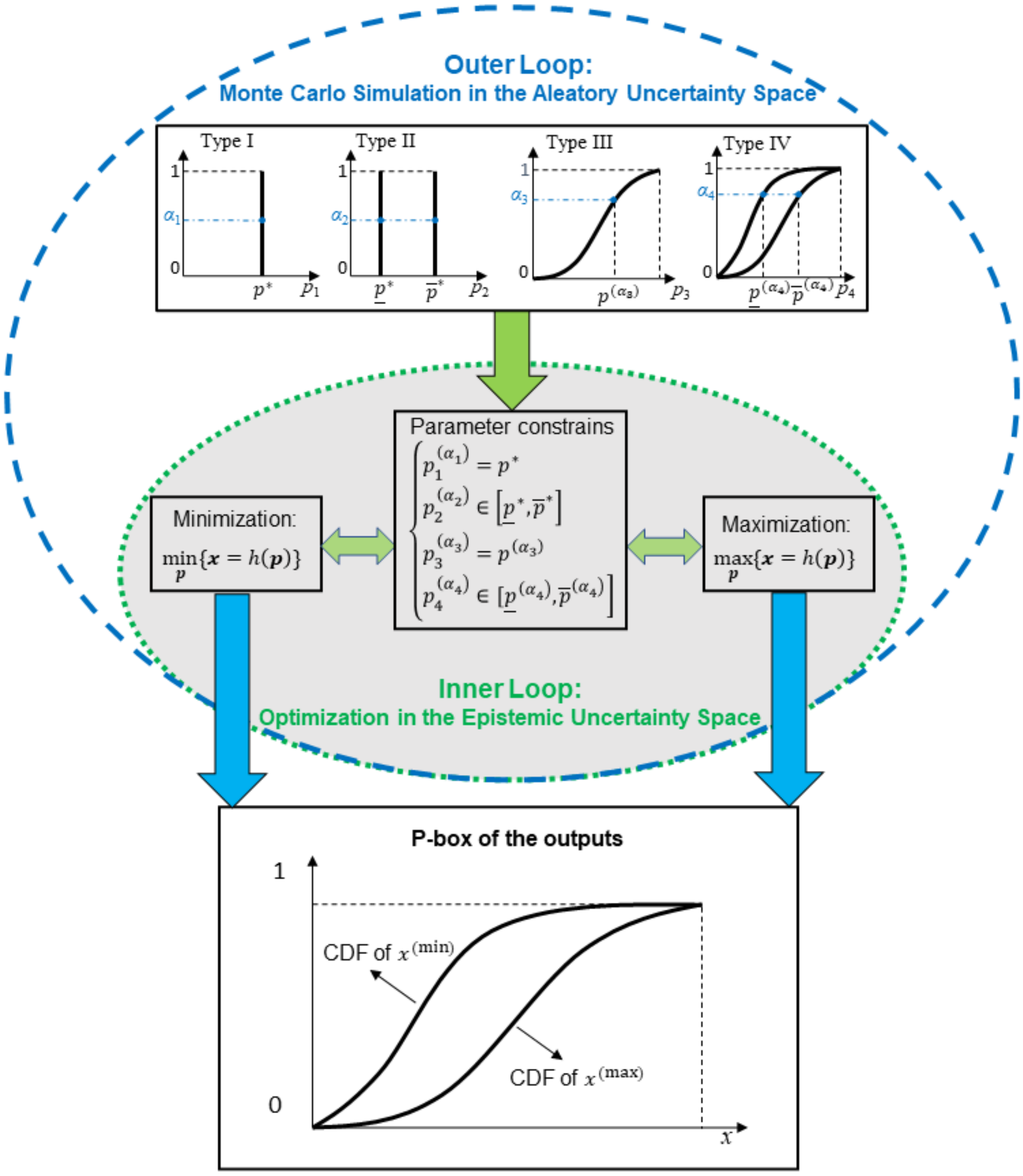

Fig. 4. The double-loop procedure for uncertainty quantification and propagation.

4.4 Basic workflow

Fig. 5 summarizes the basic workflow of the uncertainty quantification and propagation framework. The first step is to categorize all input parameters into Type I /II /III / IV according to whether the aleatory and/or epistemic uncertainties are involved, as stated in subsection 4.1. In this study, the inputs include both the structure and the excitation parameters. Detailed descriptions of uncertainty characteristics of the input parameters are provided in subsection 5.3. Next, the double-loop procedure is performed to quantify and propagate the uncertainties from inputs to outputs in the form of P-box (Fig. 4). The main model of the simulator is the calculation model from crowd-induced load to structural response calculation (see section 2 and 3). Then, the P-box of the outputs is obtained. The outputs can be interested parameters in vibration serviceability assessments, e.g., the maximum acceleration responses of the structure (see section 3).

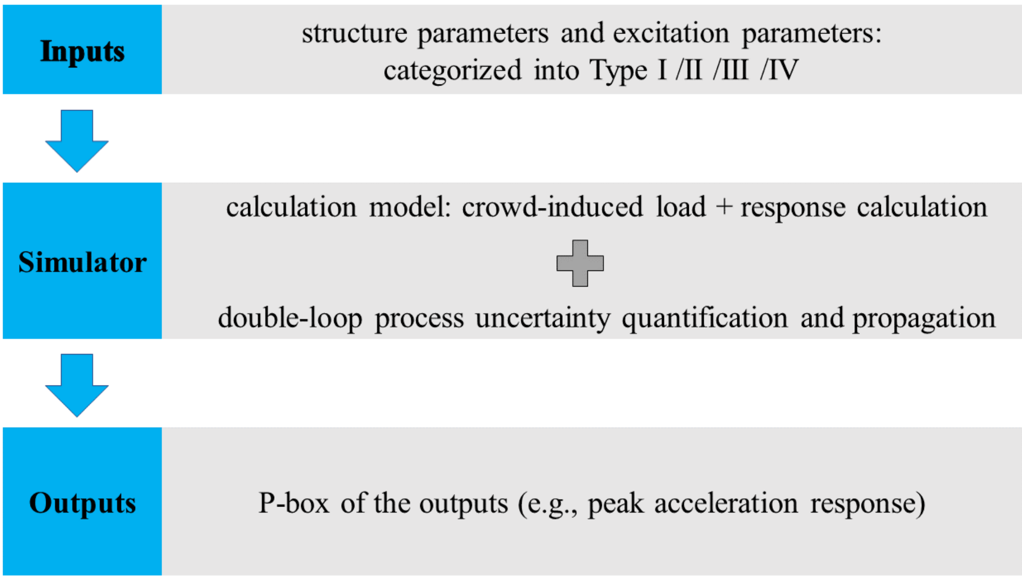

Fig. 5. Basic workflow.

5. An illustrative example

5.1 Structural parameters

A footbridge with 30 m length and 3 m width is considered as an illustrative example. The coordinate system and dimensions are set the same as shown in Fig. 2. In current example, the considered footbridge is a simply supported Bernoulli beam structure. Correspondingly, its fundamental bending mode in vertical (Z) direction is relevant and considered. The modal shape is sinusoidal with $\emptyset_n = \sin(\pi x/L)$. The modal mass is $M_n = 20$ tons. The structure has a nominal (mean) natural frequency of $\bar{f}_n = 2$ Hz. The nominal damping ratio is $\bar{D}_n = 0.01$. As stated in Section 3, the actual values of f_n and D_n may vary and thus respectively considered as variable within intervals of $[0.9\bar{f}_n, 1.1\bar{f}_n]$ Hz and $[0.5\bar{D}_n, 1.5\bar{D}_n]$.

5.2 Excitation parameters

The example considers a uni-directional Asian crowd with commuter purpose. The density is set as $d = 0.2$ persons/m², corresponding to weak traffic as defined in (HiVoSS 2008 and Sétra 2006). The adjusting coefficients are set as: for geographic area, $\alpha_\mathrm{G} = 0.92$; and for travel purpose, $\alpha_\mathrm{T} = 1.11$ and $\gamma = 0.214 d_\mathrm{jam} = 1.156$ persons/m². Correspondingly, the mean walking speed of the crowd is $\bar{v}(d) = 1.36$ m/s and thus the initial walking speeds $v_\alpha^0(0)$ of the crowd follow the Normal distribution: $\mathcal{N}(1.36, 0.26)$ m/s. The arrival times $t_{\mathrm{arr},\alpha}$ follow a Poisson distribution with $\lambda = 8.18$ persons/s. The initial positions in lateral (Y) direction Y_α^0 are random values following the Uniform distribution: $U(0.3, 2.7)$ m. The pedestrian body weights G_α follow a Normal distribution: $\mathcal{N}(750,150)$ N, as reported in (Živanović 2012).

5.3 Uncertainty characteristics of input parameters

According to the principles as stated in section 4.1, the structure and excitation parameters for the current illustrative example are categorized into four types. More detailed descriptions are summarized in Table 2 and Table 3. The basic categorization information is listed as follows:

- Type I parameters (constant values): L, W, d, α_{G}, α_{T}, γ, M_n, $\emptyset_n$;
- Type II parameters (constants within a known interval): f_n, D_n;
- Type III parameters (described with fully determined probability distribution): $t_{\mathrm{arr},\alpha}$, Y_α^0, $v_\alpha^0(0)$, G_α;
- Type IV parameters (imprecise probability variables with only vaguely determined uncertainty characteristics): $\vec{v}_\alpha(t)$, $\vec{r}_\alpha(t)$, $v_{s,\alpha}$, $f_{s,\alpha}$, $DLF_{z,\alpha,1}$, $DLF_{z,\alpha,2}$, $DLF_{z,\alpha,3}$, $DLF_{z,\alpha,4}$.

It is notable that, some parameters are indirect input parameters, i.e., $\vec{v}_\alpha(t)$, $\vec{r}_\alpha(t)$, $v_{s,\alpha}$, $f_{s,\alpha}$, $DLF_{z,\alpha,1}$, $DLF_{z,\alpha,2}$, $DLF_{z,\alpha,3}$, and $DLF_{z,\alpha,4}$, are determined by other input parameters:

$$\vec{v}_\alpha(t) = F_1(L, W, d, \alpha_{\mathrm{G}}, \alpha_{\mathrm{T}}, \gamma, t_{\mathrm{arr},\alpha}, Y_\alpha^0, v_\alpha^0(0)) \tag{23a}$$

$$\vec{r}_\alpha(t) = F_2(L, W, d, \alpha_{\mathrm{G}}, \alpha_{\mathrm{T}}, \gamma, t_{\mathrm{arr},\alpha}, Y_\alpha^0, v_\alpha^0(0)) \tag{23b}$$

$$v_{s,\alpha} = F_3(L, W, d, \alpha_{\mathrm{G}}, \alpha_{\mathrm{T}}, \gamma, t_{\mathrm{arr},\alpha}, Y_\alpha^0, v_\alpha^0(0)) \tag{23c}$$

$$f_{s,\alpha} = F_4(v_{s,\alpha}) \tag{23d}$$

$$DLF_{z,\alpha,1} = F_5(f_{s,\alpha}) \tag{23e}$$

$$DLF_{z,\alpha,2} = F_6(f_{s,\alpha}) \tag{23f}$$

$$DLF_{z,\alpha,3} = F_7(f_{s,\alpha}) \tag{23g}$$

$$DLF_{z,\alpha,4} = F_8(f_{s,\alpha}) \tag{23h}$$

where '$Outputs = F_k(Inputs)$' represents the '$Outputs$' is a function of '$Inputs$', i.e., the '$Outputs$' depend on the '$Inputs$'.

Thus, the peak acceleration response a_{peak} depends on and can be formulated by the direct input parameters, as:

$$a_{peak} = F(L, W, M_n, f_n, D_n, \emptyset_n, d, \alpha_{\mathrm{G}}, \alpha_{\mathrm{T}}, \gamma, t_{\mathrm{arr},\alpha}, Y_\alpha^0, v_\alpha^0(0), G_\alpha) \tag{24}$$

Table 2: The uncertainty characteristics of direct input parameters for crowd behaviour simulation.

Sub-models	Parameter	Category	Distribution	Uncertainty characteristics
Structure	L	I	Constant	Fixed value for a given structure, e.g., 30 m
	W	I	Constant	Fixed value for a given structure, e.g., 3 m
Crowd	d	I	Constant	Fixed value applied in vibration serviceability assessments, e.g., 0.1, 0.2, 0.5, 0.8, 1.0, 1.5 persons/m^2 (HiVoSS 2008 and Sétra 2006)
	α_{G}	I	Constant	Fixed value for known geographic area, e.g., $\alpha_{\mathrm{G}} = 0.92$ for Asian crowds.
	α_{T}	I	Constant	Fixed value for given travel purpose, e.g., $\alpha_{\mathrm{T}} = 1.11$ for Commuters.
	γ	I	Constant	Fixed value for given travel purpose, e.g., $\gamma = 0.214 d_{\mathrm{jam}} = 1.156$ persons/m^2 for Commuters.
	$t_{\mathrm{arr},\alpha}$	III	Poisson	$\lambda = W \cdot d \cdot \bar{v}(d) = 30 \cdot 0.2 \cdot 1.3632 = 8.18$ persons/s (Živanović 2012, Wei et al. 2017 and Fu and Wei 2020) in the considered example
	Y_α^0	III	Uniform	$Y_\alpha^0 \sim U(r_\alpha, W - r_\alpha) = U(0.3, 2.7)$ m (Wei et al. 2017 and Fu and Wei 2020)
	$v_\alpha^0(0)$	III	Normal	$v_\alpha^0(0) \sim \mathcal{N}(\mu_{vs}, \sigma_{vs}) = \mathcal{N}(1.36, 0.26)$ m/s (Helbing et al. 1995, 2000a, Wei et al. 2017 and Fu and Wei 2020)

Table 3: The uncertainty characteristics of direct and indirect input parameters for structural response calculation.

Sub-models	Parameter	Category	Distribution	Uncertainty characteristics
Structure	L	I	Constant	Fixed value for a given structure, e.g., 30 m
	W	I	Constant	Fixed value for a given structure, e.g., 3 m
	f_n	II	Constant	Constant within interval $[0.9\bar{f_n}, 1.1\bar{f_n}]$ (Lievens et al. 2016)
	D_n	II	Constant	Constant within interval $[0.5\bar{D}_n, 1.5\bar{D}_n]$ (Lievens et al. 2016)
	M_n	I	Constant	Fixed value for a specific mode of a given structure, e.g., 20 tons
	$\emptyset_n$	I	Constant	Keep constant for a specific mode of a given structure, e.g., sinusoidal with $\emptyset_n = \sin(\pi x/L)$
Crowd	$\vec{v}_\alpha(t)$	IV	Unknown	Indirectly output from crowd behaviour simulation
	$\vec{r}_\alpha(t)$	IV	Unknown	Indirectly output from crowd behaviour simulation
	$v_{s,\alpha}$	IV	Unknown	Indirectly output from crowd behaviour simulation
Excitation	G_α	III	Normal	$G_\alpha \sim \mathcal{N}(\mu_G, \sigma_G) = \mathcal{N}(750, 150)$ N (Živanović 2012)
	$f_{s,\alpha}$	IV	Unknown	Indirectly derived from the outputs of crowd behaviour simulation, using the step frequency-speed relation (Eq. (14)).
	$DLF_{z,\alpha,1}$	IV	Unknown	Indirectly derived by (Eq. (16a)).
	$DLF_{z,\alpha,2}$	IV	Unknown	Indirectly derived by (Eq. (16b)).
	$DLF_{z,\alpha,3}$	IV	Unknown	Indirectly derived by (Eq. (16c)).
	$DLF_{z,\alpha,4}$	IV	Unknown	Indirectly derived by (Eq. (16d)).

Note: the indirect input parameters are marked with 'indirectly' and obtained before structural response calculations.

5.4 Results

5.4.1 Uncertainty characterization of the direct inputs

Fig. 6 shows the uncertainty characterization of the direct inputs. For clarity, the Type I parameters (constant values without any uncertainty) are not plotted. Clearly, Type III parameters are described as fully-determined random variables, and hence are presented as single CDF curves as shown in Fig. 6(c-f). For Type II parameters, since they contain only the epistemic uncertainty, their intervals are transferred into a special shape of P-box, whose right and left bounds are essentially two vertical CDF functions of the bounds of the intervals, as illustrated in Fig. 6(a-b). To follow the workflow (Fig. 5), 1000 random probability data points are firstly sampled during the Monte Carlo simulation in the first loop, according to the descriptions in section 5.3.

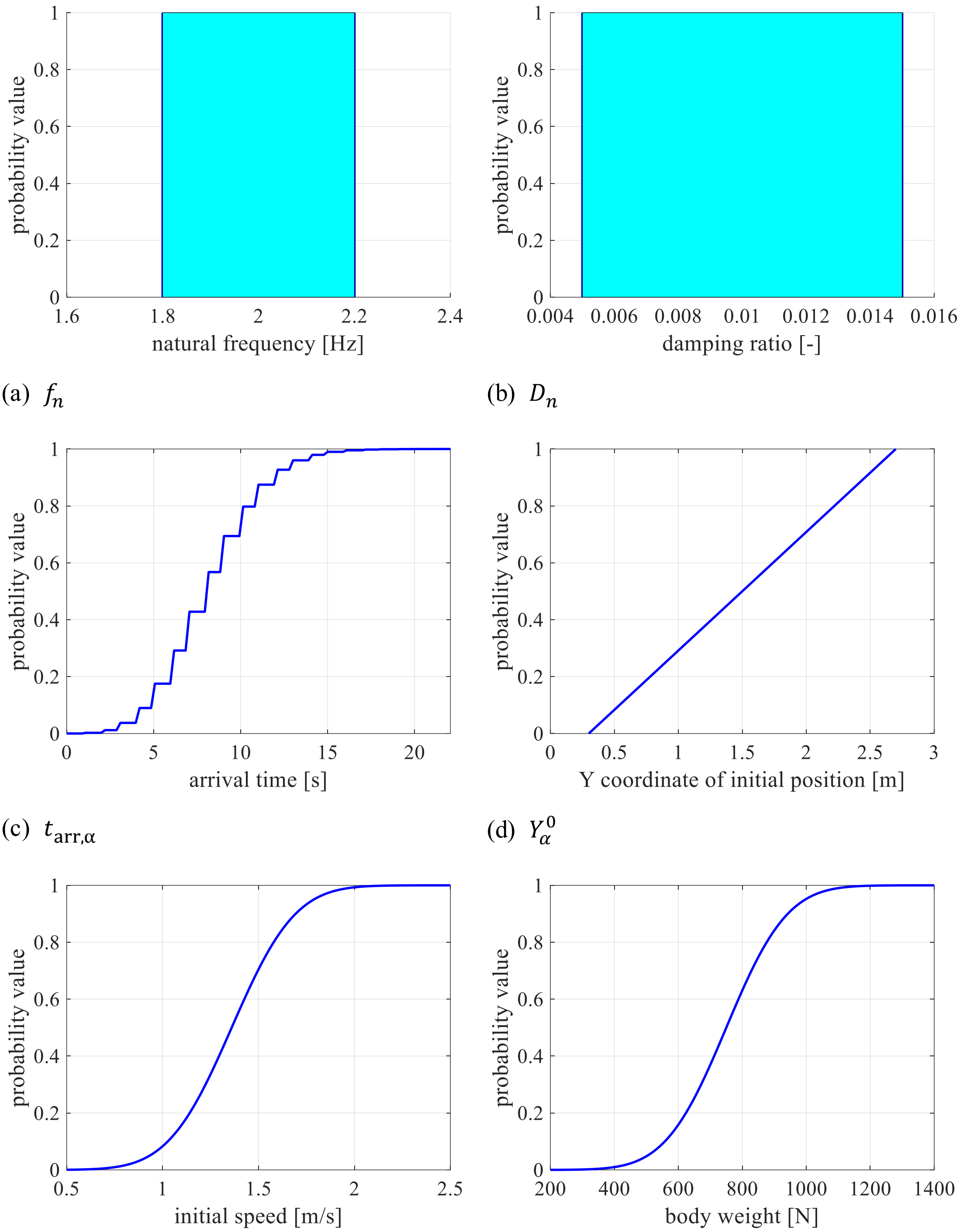

(a) f_n (b) D_n (c) $t_{\mathrm{arr},\alpha}$ (d) Y_α^0 (e) $v_\alpha^0(0)$ (f) G_α

Fig. 6. The uncertainty characterization of the direct inputs.

5.4.2 P-boxes of the intermediate parameters

After the P-boxes of the direct input parameters are determined, the whole simulator works to propagate uncertainties from the direct inputs to indirect inputs, i.e. the intermediate parameters, and finally to the outputs. Each Monte Carlo simulation corresponds to one random pedestrian crowd, which leads to one set of indirect inputs. Due to both aleatory and epistemic uncertainties of the pedestrian crowd, it leads to the uncertainties of the indirect inputs. Fig. 7 presents the corresponding P-boxes. Table 4 summarizes the mean and standard deviation of the parameters. The walking speeds of the crowds can have up to near 14% difference in mean and near 60% difference in standard deviation. The corresponding differences for step frequencies are near 6% for mean and near 79% for standard deviation. For the DLFs, the largest difference in mean occurs in the first DLF, i.e., around 12%; the differences in standard deviation are all over 75% for the first four DLFs. The differences in mean and standard deviation characterize the uncertainty spaces of the indirect inputs and may result in significant impacts on the crowd-induced loads.

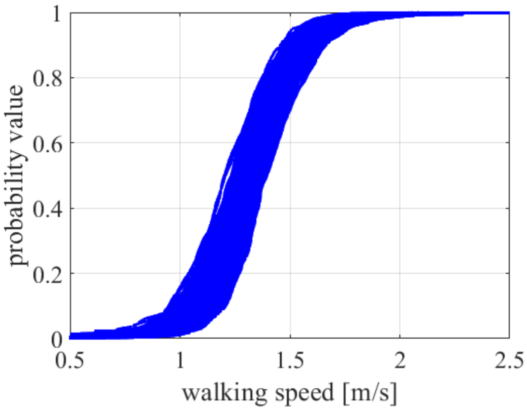

(a) $v_{s,\alpha}$

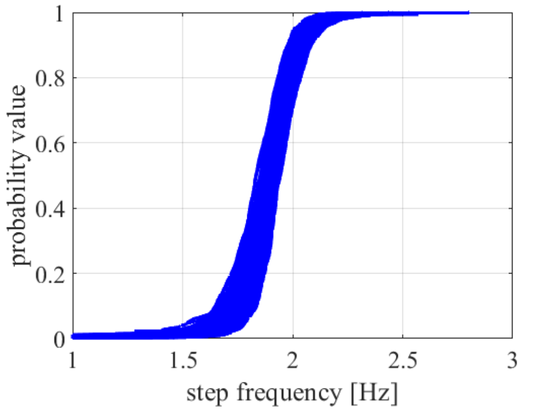

(b) $f_{s,\alpha}$

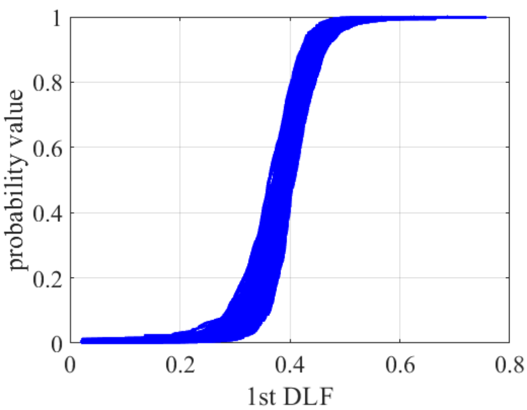

(c) $DLF_{z,\alpha,1}$

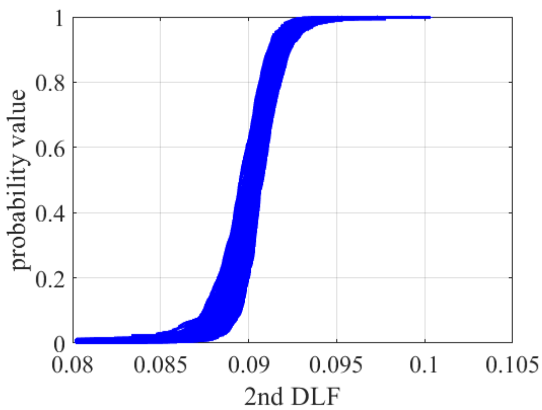

(d) $DLF_{z,\alpha,2}$

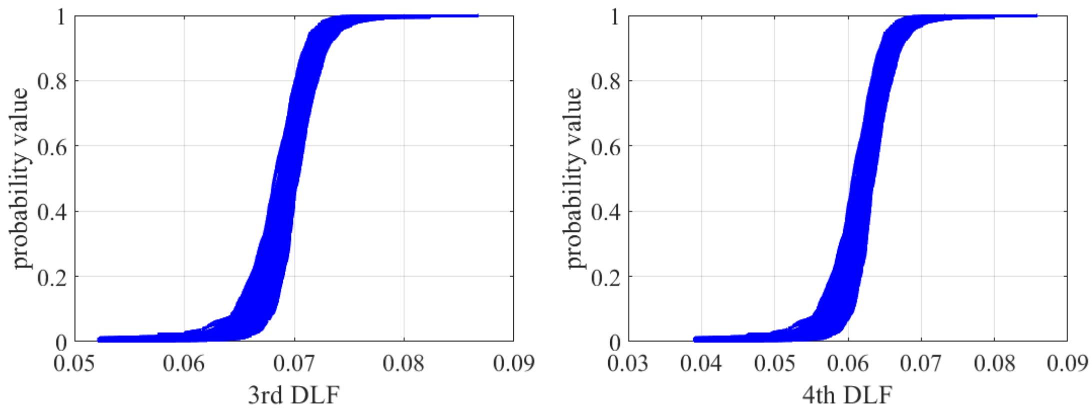

(e) $DLF_{z,\alpha,3}$ (f) $DLF_{z,\alpha,4}$

Fig. 7. The P-boxes of the intermediate parameters.

Table 4: mean and standard deviation (std) of the indirect inputs.

Parameter	**Min. mean**	**Max. mean**	**Δ [%]**	**Min. std**	**Max. std**	**Δ [%]**
$v_{s,\alpha}$ [m/s]	1.2243	1.3947	13.92	0.1635	0.2617	60.06
$f_{s,\alpha}$ [Hz]	1.8322	1.9381	5.78	0.0987	0.1768	79.13
$DLF_{z,\alpha,1}$	0.3617	0.4051	12.00	0.0405	0.0725	79.01
$DLF_{z,\alpha,2}$	0.0895	0.0907	1.34	0.0011	0.0020	81.82
$DLF_{z,\alpha,3}$	0.0682	0.0702	2.93	0.0019	0.0034	78.95
$DLF_{z,\alpha,4}$	0.0606	0.0634	4.62	0.0026	0.0046	76.92

5.4.3 P-boxes of outputs

By following the workflow (Fig. 5), the uncertainties of the direct and indirect inputs are propagated to the final outputs in the double-loop process (Fig. 4). During the process, for each Monte Carlo sampling, the inner loop executes the optimization to determine the maximum and minimum of the peak acceleration. Totally, 1000 Monte Carlo simulations are performed. Fig. 8 presents the P-box of the peak accelerations, which shows a clear representation of the uncertainty space of the peak acceleration responses of the footbridge. The lower border of the P-box represents the CDF of the minimum peak accelerations, which ranges from near 0.5 to 1.5 m/s^2. The upper boundary, i.e., the CDF of the maximum peak accelerations, is much widely distributed from near 0.5 to 3.0 m/s^2. The significantly large uncertainty space of the peak accelerations results from the effects of both the footbridge dynamic model and the uncertain crowd-induced loads on the structural responses. According to (e.g., HiVoSS 2008), the lower and upper borders may correspond to significantly different comfort classes. Correspondingly, the failure probability of each comfort class is different (Table 5). For instance, the exceedance probability of the medium acceleration limit for the lower and the upper borders are 43% and 94%, respectively.

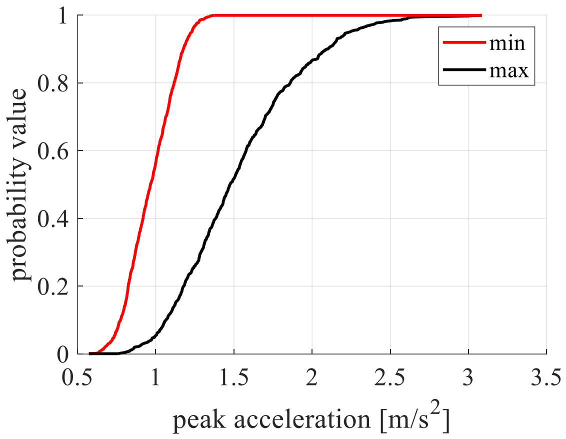

Fig. 8. The P-box of the peak acceleration.

Table 5: failure probability of each comfort class according to (HiVoSS 2008).

comfort class	**comfort degree**	**acceleration limit [m/s^2]**	**failure probability**
CL 1	maximum	0.50	100% for both borders
CL 2	medium	1.00	43% for lower border 94% for upper border
CL 3	minimum	2.50	0% for lower border 2% for upper border

6. Conclusions

This paper proposes a comprehensive framework to quantify and propagate the uncertainties from both the structure dynamic model and the crowd-induced load to the acceleration responses of footbridges. The social force model is proposed to characterize the crowd behaviour. By combining with a single pedestrian induced walking force model, the crowd behaviour is translated to the crowd-induced load. The structure dynamic model is constructed by decoupling the continuous model into several single degrees of freedom systems according to relevant modes in the vibration serviceability evaluation. Together with the crowd-induced load model, structural responses are calculated. Specifically, the interested peak acceleration is identified for each simulation.

For the uncertainty analysis, a double-loop framework is formulated to investigate all the uncertain parameters and to perform uncertainty quantification and propagation in the form of P-box. Meanwhile, the uncertainty space of the peak structural responses is obtained by the Monte Carlo sampling and optimization in the outer loop and inner loop, respectively.

The feasibility and performance of the overall approach are demonstrated by an illustrative example, where the failure probability of each comfort class regarding the peak acceleration response is also evaluated. Results show that, random crowd behaviour (direct inputs) firstly result in large scatter in excitation parameters (indirect inputs), e.g., walking speeds, step frequencies, dynamic load factors, etc. These differences finally lead to significantly large uncertainty space of the peak accelerations of the structure (outputs). Results also indicate special attention should be paid on both the epistemic and aleatory uncertainties from the crowd behaviour in the vibration serviceability assessments of footbridges. Furthermore, the proposed uncertainty quantification framework may provide significant insights and improve the reliability for future vibration serviceability evaluations of footbridges by incorporating the crowd behaviour effects.

Acknowledgements

This work is supported by the National Natural Science Function of China (grant no. 12102036). The third author is supported by the Alexander von Humboldt Foundation (award No. 1193706) and the Beijing Institute of Technology Research Fund Program for Young Scholars, which are greatly appreciated.

References

Alexander N., Theoretical treatment of crowd-structure interaction dynamics, *Structures and Buildings*, vol. 159, pp. 329-338, 2006.

Alvarez, D.A., Reduction of uncertainty using sensitivity analysis methods for infinite random sets of indexable type, Int. J. Approx. Reason. 50 (2009) 750–762, https://doi.org/10.1016/J.IJAR.2009.02.002.

Behmanesh, I; Yousefianmoghadam, S; Nozari, A; Moaveni, B; Stavridis, A. (2018). Uncertainty quantification and propagation in dynamic models using ambient vibration measurements, application to a 10-story building, *Mechanical Systems and Signal Processing*, 107, 502-514.

Ben Abdessalem, A., Jenson, F., Calmon, P.. (2018). Quantifying uncertainty in parameter estimates of ultrasonic inspection system using Bayesian computational framework, *Mechanical Systems and Signal Processing*, 109, 89-110.

Bi, S., Broggi, M., Wei, P., Beer M. The Bhattacharyya distance: Enriching the P-box in stochastic sensitivity analysis. *Mechanical Systems and Signal Processing* 129 (2019) 265–281.

Borges, RA; Rodovalho, LFF; Sales, TD; Rade, DA. (2021). Stochastic eigenfrequency and buckling analyses of plates subjected to random temperature distributions, *Mechanical Systems and Signal Processing*, 147, 107088.

Bruno, L., Venuti, F. (2008). The pedestrian speed-density relation: modelling and application, *Footbridge2008*, July, Porto, Portugal.

Buchmueller, S., Weidmann, U. Parameters of pedestrians, pedestrian traffic and walking facilities. Technical Report, no. 132; 2006.

Chopra, A. Dynamics of Structures: Theory and Applications to Earthquake Engineering (fourth edition), New Jersey: Prentice-Hall Inc, 2012.

Díaz, IM, Reynolds, P, (2010). On-off nonlinear active control of floor vibrations, *Mechanical Systems and Signal Processing*, 24(6), 1711-1726.

Ferreira, F.; Moutinho, C.; Cunha, A.; Caetano, E.. (2019). Use of semi-active tuned mass dampers to control footbridges subjected to synchronous lateral excitation. *Journal of Sound and Vibration*, 446, 176-194.

Ferson, S., Kreinovich, V., Ginzburg, L., Myers, D.S., Sentz, K. Constructing Probability Boxes and Dempster-Shafer Structures, Sandia National Laboratories Report, SAND2002-4015, 2003. doi: 10.2172/809606

Fu, B., Wei, X. An intelligent analysis method for human-induced vibration of concrete footbridges. *International Journal of Structural Stability and Dynamics*, 21(01), 2150013: 1-26, November 2020.

Geweth, CA; Baydoun, SK; Saati, F; Sepahvand, K; Marburg, S. (2021). Effect of boundary conditions in the experimental determination of structural damping, *Mechanical Systems and Signal Processing*, 146, 107052.

Gong M., Li Y., Shen R. and Wei X. “Glass suspension footbridge: human-induced vibration, serviceability evaluation, and vibration mitigation.” *Journal of Bridge Engineering*, 26 (11): 05021014. https://doi.org/10.1061/(ASCE)BE.1943-5592.0001788.

Helbing, D., Buzna, L., Johansson, A., Werner, T., Johansson, A., and Werner, T. (2005). “Self-Organized Pedestrian Crowd Dynamics: Experiments , Simulations , and Design Solutions.” *Transportation Science* 39(1): 1-24.

Helbing, D., Farkas, I., Vicsek, T. Simulating dynamical features of escape panic, *Nature* **794** (2000) 487–490.

Helbing, D., Molnar, P. Social force model for pedestrian dynamics, *Phys. Rev. E* **51** (1995) 4282–4286.

HiVoSS. (2008). Human induced Vibrations of Steel Structures - Design of Footbridges Guideline. *Research Fund for Coal and Steel*.

International Standard (ISO), ISO 10137: Bases for design of structures – serviceability of buildings and walkways against vibrations, 2007.

Jiang, Y., Zhou, H., Wang, L., Chen, Z., Tang, T., Adhikari, S. (2021). Reliability Evaluation Based on Multiple Response Surfaces Method Considering Construction Uncertainties of Cable Tension for a Hybrid Roof Structure, *ASCE-ASME Journal of Risk and Uncertainty in Engineering Systems, Part A: Civil Engineering*, 7(3): 04021033.

Kareem, A., Gurley, K. Damping in structures: Its evaluation and treatment of uncertainty. *Journal of Wind Engineering and Industrial Aerodynamics*, 59(2–3), 131–157, 1996.

Kwon, K., Ryu, N., Seo, M., Kim, S., Lee, T., Min, S. (2020). Efficient uncertainty quantification for integrated performance of complex vehicle system, *Mechanical Systems and Signal Processing*, 139, 106601.

Lievens, K., Lombaert, G., De Roeck, G., Van den Broeck, P. Robust design of a TMD for the vibration serviceability of a footbridge, *Engineering Structures*, 123(2016) 408-418.

Mohammed A. and Pavic A., Human-structure dynamic interaction between building floors and walking occupants in vertical direction, *Mechanical Systems and Signal Processing*, vol. 147, p. 107036, 2020.

Moser, P., Moaveni, B. Environmental effects on the identified natural frequencies of the Dowling Hall Footbridge, *Mechanical Systems and Signal Processing*, 25(7), 2336-2357, 2011.

Sétra, Footbridges: assessment of vibrational behaviour of footbridges under pedestrian loading, *AFGC (Association Française de Génie Civil)*, Afgc, Paris, 2006.

Vishwanathan, A.; Vio, GA. (2019). Numerical and experimental assessment of random matrix theory to quantify uncertainty in aerospace structures, *Mechanical Systems and Signal*

Processing, 118, 408-422.

Wei, X. A simplified method to account for human-human interaction in the prediction of pedestrian-induced vibrations. Struct Control Health Monit. 2021;e2753. https://doi.org/10.1002/stc.2753.

Wei, X., Van Den Broeck, P., De Roeck, G., Van Nimmen, K. A simplified method to account for the effect of human-human interaction on the pedestrian-induced vibrations of footbridges, *Procedia Eng.* **199** (2017) 2907–2912.

Weidmann, U. Transporttechnik der fussganger. Ivt Report, no. 90; 1993.

Xia, Y., Hao, H., Zanardo, G., Deeks, A. Long term vibration monitoring of an RC slab: Temperature and humidity effect, *Engineering Structures*, 28(3), 441-452, 2006.

Young, P. Improved floor vibration prediction methodologies, Proceedings of Arup Vibration Seminar on Engineering for Structure Vibration: Current Developments in Research and Practice, London, 2001.

Zhang, H. Nondeterministic linear static finite element analysis: an interval approach. PhD thesis, Georgia Institute of Technology, USA, 2005.

Zhang, H., Mullen, RL, Muhanna, RL. (2010). Interval Monte Carlo methods for structural reliability. *Structural Safety*, 32(3), 183-190.

Živanović, S., Pavic, A., Reynolds P. (2005). Vibration serviceability of footbridges under human-induced excitation: a literature review. *Journal of Sound and Vibration*, 279 (1-2), 1-74.

Živanović, S. (2012). Benchmark Footbridge for Vibration Serviceability Assessment under Vertical Component of Pedestrian Load. *ASCE Journal of Structural Engineering*, 138 (10), 1193-1202.